Available online at www.sciencedirect.com
ScienceDirect
Carbohydrate Polymers 71 (2008) 263–268
Carbohydrate Polymers
www.elsevier.com/locate/carbpol

The structure and properties of a starch-based biodegradable film

HanGuo Xiong *, ShangWen Tang [1], HuaLi Tang [2], Peng Zou [2]

College of Food Science and Technology, Huazhong Agricultural University, Wuhan 430070, China

Received 23 April 2007; received in revised form 24 May 2007; accepted 24 May 2007
Available online 7 June 2007

Abstract

A starch-based biodegradable film, with a nano silicon dioxide (nano-SiO_2) content, was prepared by the coating method in this paper, through which its physical and biodegradable properties were studied. The structure of the film was characterized by Fourier transform infrared spectroscopy (FT-IR), X-ray photoelectron spectroscopy (XPS), X-ray diffraction (XRD), differential scanning calorimeter (DSC), and scanning electron microscopy (SEM). As compared to a film without nano-SiO_2, the crystallinity of the film was decreased from 41.2% to 32.9%; the tensile strength, breaking elongation, and transmittance were increased by 79.4%, 18%, and 15%, respectively; and the water absorption was decreased by 70%. A hydrogen bond was formed in nano-SiO_2 and starch/polyvinyl alcohol (PVA), and intermolecular hydrogen bonding of the starch was decreased at the addition of nano-SiO_2. Meanwhile, the chemical bond C–O–Si was also formed in nano-SiO_2/starch/PVA hybrid materials; therefore, the miscibility and compatibility between starch and PVA were increased.

Keywords: Corn starch; Biodegradable film; Structure; Properties

1. Introduction

Recently, environmentally friendly materials from natural and renewable resources have received much attention (Ma & Yu, 2004; Nakamura, Cordi, Almeida, Duran, & Mei, 2005; Yu, Dean, & Li, 2006). Starch, as an abundant raw material with low cost, has been applied in the field of degradable plastics, and blend films containing starch are potential materials in the agriculture, medicine, and packaging industries (Funke, Bergthaller, & Lindhauer, 1998; Hulleman, Janssen, & Feil, 1998; Lu, Tighzerta, Dole, & Erre, 2005). To improve the mechanical properties of materials, blending starch with other polymers such as polymethylcellulose and low-density polyethylene is regarded as the simplest way.

Starch blended with synthetic polymer polyvinyl alcohol (PVA) has been studied as a potential biodegradable polymer (Follain, Joly, Dole, & Bliard, 2005; Xiao & Yang, 2006; Zhai, Yoshii, Kume, & Hashim, 2002; Zhai, Yoshii, & Kume, 2003). Depending on the degree of biodegradability, it seems that PVA might provide a stable support medium for starch films (Jayasekara, Harding, Bowater, Christie, & Lonergan, 2004). The mechanical properties and biodegradability of starch/PVA blended films have been reported by several researchers. However, their wide applications are limited by the lack of water resistance and the poor mechanical property of starch/PVA blended films (Bikiaris et al., 1998).

In this study, the starch/PVA blended films were modified by nano-SiO_2. Nano-SiO_2 is a kind of amorphous powder with a molecular structure that is a tridimensional net, the structure of which is as follows:

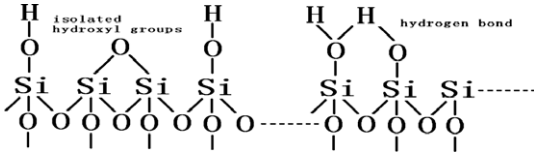

* Corresponding author. Tel.: +86 2763 215853; fax: +86 2787 286608.
E-mail addresses: xionghanguo@163.com (H. Xiong), tsw830629@webmail.hzau.edu.cn (S. Tang), tanghuali58@163.com (H. Tang), zoupeng621@163.com (P. Zou).
[1] Tel.: +86 2787 288377.
[2] Tel.: +86 2787 282533.

0144-8617/$ - see front matter © 2007 Elsevier Ltd. All rights reserved.
doi:10.1016/j.carbpol.2007.05.035

Nano-SiO_2 deviates from a stable silicon–oxygen structure for lack of oxygen in its surface. Its molecular formula is SiO_{2-x}, in which x ranges from 0.4 to 0.8. Because of its small size, large specific surface area, high surface energy, as well as a lot of unsaturated chemical bonds and hydroxyl groups on the surface, nano-SiO_2 is easy to disperse into the macromolecular chains. Many studies indicate that nano-materials can improve the performance of polymer materials such as plastic and rubber (Chaichana, Jongsomjit, & Praserthdam, 2007; Sun, Li, Zhang, Du, & Burnell-Gray, 2006; Yang et al., 2006; Zou et al., 2007), but relevant studies regarding starch polymers modified by nano-SiO_2 have not yet been reported. Nano-SiO_2 can be used to modify starch/PVA blended films for its properties of multihydroxy and high surface activity. The physical and biodegradable properties of a starch-based biodegradable film are discovered in our laboratory, and its structure is characterized by FT-IR, XPS, XRD, and SEM.

2. Experimental

2.1. Materials

Nano silicon dioxide (nano-SiO_2) was provided by the Nanometer Engineering Center of the People's Republic of China. Its particle size was 60 nm. Corn starch (starch) was provided by Huanglong Food Ltd. of Gongzhuling City (moisture content 11.7%, protein 0.23%, fat 0.075%, ash content 0.08%). Polyvinyl alcohol (PVA) was produced by the Chongqing Inorganic Chemical Reagent Factory (DP 1799 ± 50, NaOH $\leqslant 0.2\%$, acetic acid remnant $\leqslant 0.13\%$, volatilization content $\leqslant 9.0\%$, and transmissivity $\geqslant 90\%$). Hexamethylenetramine, glycerine, Tweenum-80, and liquid paraffin were all analytical grade reagents and were used as received.

2.2. Sample preparation

2.2.1. Preparation of SP film

Ten grams of starch and 4 g PVA were poured into a round bottom flask with 110 mL de-ionized water, and then it was stirred with high speed (>1000 r/min) in a constant temperature water bath at 95 °C for 20 min. Then 0.1 g hexamethylenetramine was added, and stirring was continued for another 40 min (>1000 r/min). One and a half grams of glycerine, 0.6 g Tweenum-80, and 1.2 g liquid paraffin were mixed in turn and continuously stirred for 10 min, and the mixture was cast onto a glass plate which was placed on a leveled flat surface. After the blend was allowed to dry at 95 °C in an oven for 1 h, the films were then peeled off and reserved.

2.2.2. Preparation of NSP film

Ten grams of starch and 0.3 g nano-SiO_2 were added into a bowl and were milled for 1 h for mixed uniformity. The mixture and 4 g PVA were then poured into a round bottom flask with 110 mL de-ionized water, stirred for 5 min with a high speed (>1000r/min), then dispersed for 10 min by ultrasound (intermittent dispersion of pulsing on for 3 s and off for 2 s, intension of 50%). After the high-speed stirring in a water bath at a constant temperature of 95 °C for 20 min (>1000 r/min), 0.1 g hexamethylenetramine was added and again continuously stirred for 40 min (>1000 r/min). One and a half grams of glycerine, 0.6 g Tweenum-80, and 1.2 g liquid paraffin were mixed in turn and continuously stirred for 10 min. The mixture was cast onto a glass plate, which was placed on a leveled flat surface. After the blend was allowed to dry at 95 °C in an oven for 1 h, the films were then peeled off and reserved.

2.3. Characterization

The powdered samples were blended with potassium bromide and laminated, and the IR spectra were recorded with a Nicolet (USA) Nexus 470 FT-IR spectrometer. The wave range from 4000 to 400 cm^{-1} was scanned 32 times for spectrum integration. The scanning resolution was 16 cm^{-1}.

XPS analysis was conducted using a Perkin Elmer PHI 5600 ESCA system. Setting the hydrocarbon peak maximum in the C_{1s} spectra to 284.6 eV referenced the binding energy scales for the samples.

The X-ray diffraction (XRD) curves of the SP film and NSP films were recorded with a Rigaku (Japan) D/max-RB X-ray diffractometer, and a Cu Kα target was used at 40 kV and 50 mA. The diffraction angle ranged from 60° to 5°. The crystallinities of the films were calculated by $X_c = (F_c/(F_c + F_a)) \times 100\%$, where F_c and F_a were the areas of the crystal and non-crystalline regions, respectively.

The thermal properties of the film samples with a weight of about 10 mg were performed by a DSC 200PC (NETZSCH, Germany) under a nitrogen atmosphere, with a flow capacity of 25 ml/min from 0 to 300 °C at a heating rate of 10 °C/min. The SP film and NSP film of about 100 μm thickness were coated with gold in a 0.1 T vacuum degree. The cross-section morphologies were observed on a Hitachi X-650 SEM.

2.4. Physical and biodegradable properties test

The tensile strength (σ_b) and elongation at break (ε_b) of the films were measured on an electron tensile tester, CMT-6104 (Shenzhen Sans Test Machine Co., Ltd., China), according to the Chinese standard method GB/T4456-96 (Polyethylene Blown film for packaging, 1996). The film-strips were cut into 120×15 mm strips, and the gauge length (i.e., the distance between the two clamps) was set at 80 mm, with a tensile rate (i.e., the rate of extending travel of the clamp) of 250 mm/min, a return rate (i.e., the rate of return travel of the clamp) of 200 mm/min, and the breaking load of 200 N.

The 80 × 80 mm sheet film was soaked in 25 °C water for 5 min. The weights of the dried samples (W_0) were measured directly. After drying, the swollen films were placed in desiccators with silica gel until the weights were constant (W_1), and the water solubilities (W_s) were calculated using the following equation: $W_s = (W_0 - W_1)/W_0 \times 100\%$.

The percentage of light transmittance (T) of the films was measured by using a Shimadzu UV-160A spectroscope (Shimadzu, Kyoto, Japan) at 480 nm (Bangyekan, Aht-Ong, & Srikulkit, 2006). The biodegradation rate of the film was according to the methods indicated in IDT ISO 14855:1999.

3. Results and discussion

3.1. FT-IR analysis

The IR spectra of nano-SiO_2 (A), starch (B), SP film (C), and the NSP films (D) are shown in Fig. 1. The strong and wide absorption band at 3437 cm^{-1} of the nano-SiO_2 (A) samples indicated that there was plenty of –OH on the surface of the nano-SiO_2. The maximal absorptions at 1093, 802, and 468 cm^{-1} were attributed to an antisymmetric stretching vibration, symmetric stretching vibration, and flexural libration vibration of Si–O–Si, respectively.

From the spectra of starch (B), the strong and broad absorption peak at 3403 cm^{-1} was assigned to the characteristic absorption peak of the stretching vibration of –OH. The bands at 1158 and 1081 cm^{-1} were attributed to the stretching vibration of C–O in C–O–H groups and the band at 1016 cm^{-1} was attributed to the stretching vibration of C–O in C–O–C groups. Meanwhile, the characteristic absorptions of starch also appeared at 1455, 1388, and 851 cm^{-1}.

From the spectra of the SP film (C), the strong and broad absorption peak at 3429 cm^{-1} was assigned to the characteristic absorption peak of the stretching vibration of –OH. The bands at 1154 and 1081 cm^{-1} were attributed to the stretching vibration of C–O in C–O–H groups, and the band at 1028 cm^{-1} was attributed to the stretching vibration of C–O in C–O–C groups.

In IR spectra (D), the absorption peak of –OH was at 3425 cm^{-1} for the NSP films, and the peak shifted to a wave-number lower by 12 cm^{-1} than that of nano-SiO_2. The bands at 1159 and 1089 cm^{-1} were attributed to the stretching vibration of C–O in C–O–H groups, and the band at 1032 cm^{-1} was attributed to the stretching vibration of C–O in C–O–C groups. All peaks shifted to a higher wave-number than that of starch. This indicated that new hydrogen bonds were formed in the nano-SiO_2 and starch/PVA.

3.2. XPS analysis

X-ray photoelectron spectroscopy (XPS) was used to characterize nano-SiO_2, the SP film, the NSP films, and the XPS spectra, as shown in Figs. 2 and 3, By peak fitting, the binding energy and chemical state of C, O, and Si in the films are shown in Table 1.

Fig. 2 shows the wide-scan XPS spectra (from 0 to 600 eV) for nano-SiO_2, the SP films, and the NSP films. The SP film had two main absorption peaks at about 285 and 532.95 eV corresponding to C_{1s} and O_{1s}, respectively, but the NSP films had four absorption peaks at about 284.6, 532.3, 101.9, and 151.9 eV corresponding to C_{1s}, O_{1s}, Si_{2p}, and Si_{2s}, respectively. Fig. 3 shows the Si_{2p} spectrogram of nano-SiO_2 and NSP films, as compared to that of pure nano-SiO_2, from which it can be seen that the binding energy of Si_{2p} in NSP films decreased by 1.6 eV. It was suggested that the chemical environment of Si in the NSP films had been changed.

From Table 1, it could be seen that the binding energy at around 283.2, 284.6, and 286.5 eV for C_{1s} in NSP films and their corresponding chemical state were C–O–Si, C–C

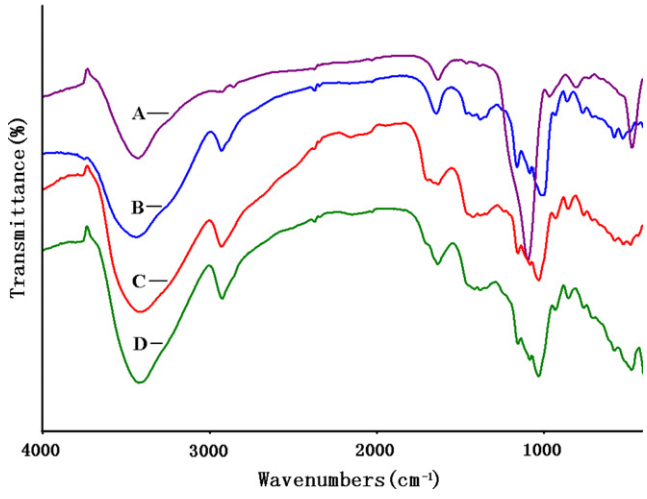

Fig. 1. IR spectrum of nano-SiO_2 (A), Starch (B), SP film (C), and NSP film (D).

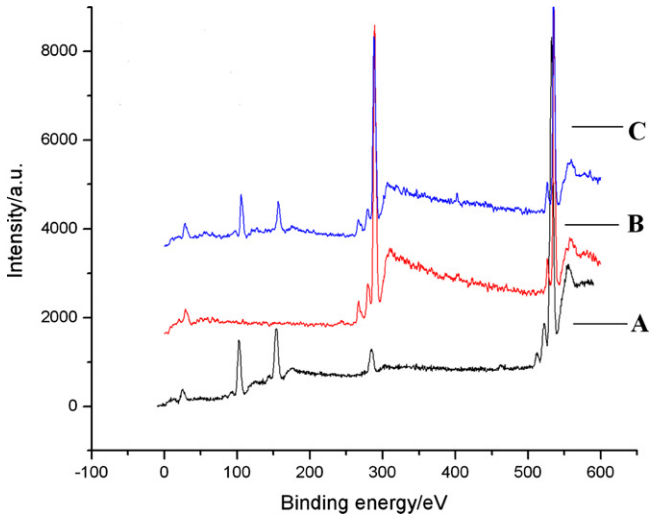

Fig. 2. XPS survey spectra of nano-SiO_2 (A), SP film (B), and NSP film (C).

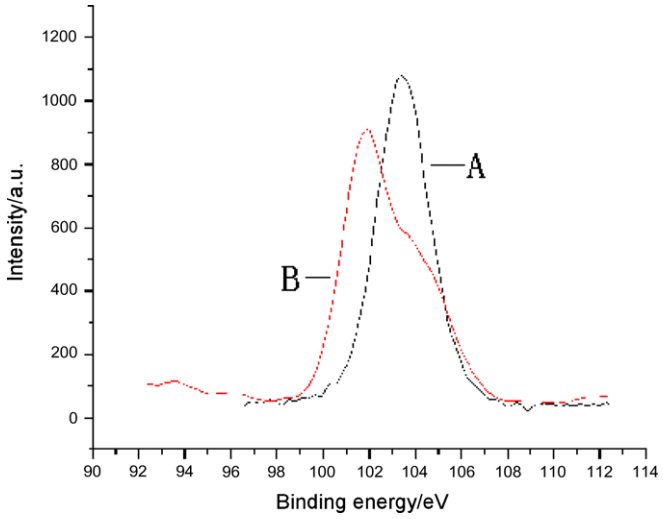

Fig. 3. Si_{2P} spectra of nano-SiO_2 (A) and NSP film (B).

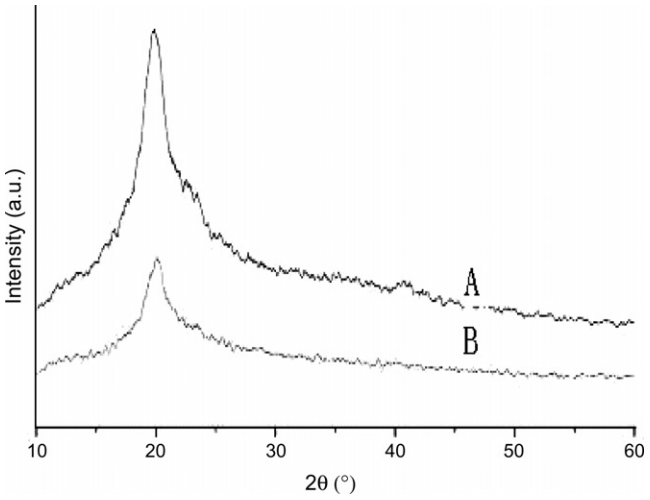

Fig. 4. X-ray diffraction patters of SP film (A) and NSP film (B).

Table 1
Binding energy and chemical state of C, O, and Si in the film

Sample	Element	Binding energy/eV	Chemical state
Nano-SiO_2	Si	103.5	Si–O
SP film	C	284.6	C–C, C–H
		286.5	C–O–H, C–O–C
	O	531.76	C–O–H
		533.27	C–O–C
NSP film	C	283.2	C–O–Si
		284.6	C–C, C–H
		286.5	C–O–H, C–O–C
	O	530.95	C–O–Si
		531.76	C–O–H
		533.27	C–O–C
	Si	101.9	Si–O–C

Table 2
Crystal properties of film by X-ray diffraction

Sample	Location 2θ/°	Relative intensity I/%	Interplanar crystal spacing d/Å	Crystallinity Xc/%
SP film	19.76	100	4.4891	41.20
	19.96	98	4.4446	
	20.30	93	4.3709	
	23.40	48	3.7984	
NSP film	17.18	53	5.1571	32.97
	19.06	84	4.6524	
	19.40	100	4.5716	
	20.82	74	4.2629	
	21.06	70	4.2149	
	21.42	72	4.1448	
	21.90	67	4.0551	

(or C–H), and C–O–H (or C–O–C), respectively. Analyzing the states of oxygen showed that the binding energy at around 530.95, 531.76, and 533.27 eV for O_{1s} in NSP films and their corresponding chemical state were C–O–Si, C–O–H, and C–O–C, respectively. As compared to the NSP film, there was no C–O–Si bond in the SP film. By combining all the XPS analysis results, the C–O–Si bond was formed in the nano-SiO_2/starch/PVA hybrid materials.

3.3. XRD analysis

From Fig. 4 and Table 2, the SP films showed a crystal sharp diffraction peak at around $2\theta = 19.76°$, 19.96°, and 20.30°. The corresponding interplanar distances calculated by the Bragg equation were 0.4489, 0.4445, and 0.4371 nm, respectively. In contrast, the NSP film also showed a crystal sharp diffraction peak at around $2\theta = 19.4°$, 19.06°, and 20.82°, and their corresponding interplanar distances were 0.4572, 0.4652, and 0.4263 nm, respectively. It was indicated that the addition of nano-SiO_2 had no influence on the crystal type of the film, but the intension and crystallinity of the diffraction peak decreased. Moreover, by calculation, the crystallinity of the NSP film decreased from 41.20% to 32.97%. Because of the effect of small size, nano-SiO_2 is easy to disperse into the macromolecular chains and form a hydrogen bond with starch and PVA, which disturbs the parallel direction of the starch/PVA chains. It was difficult for the remaining residual stress to generate induced crystallization during processing, and the crystallinity of the film decreased.

3.4. DSC analysis

From Fig. 5, there were two endothermic melting peaks in the SP films and only one endothermic melting peak in the NSP films. That is to say, the endothermic melting peak changed from double to single during 200–250 °C at the addition of the nano-SiO_2, which indicated that the miscibility of starch and PVA obviously increased. Meanwhile, as compared to the SP film, the melting temperature of the NSP film increased. This was because the hydrogen bond and chemical bond C–O–Si were generated in nano-SiO_2 and starch/PVA, which played the role of

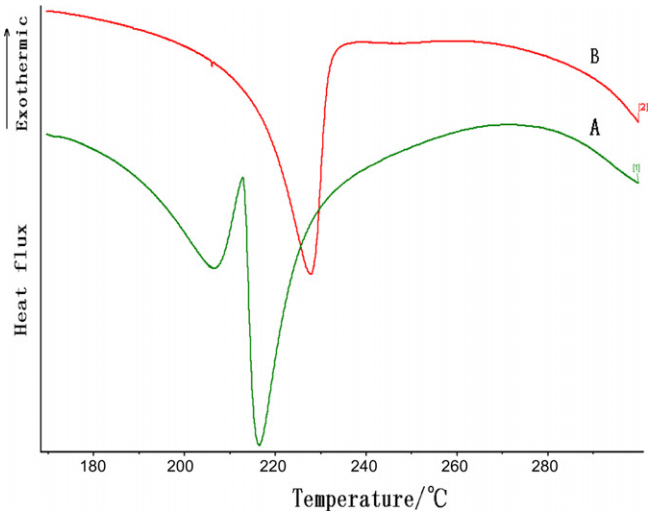

Fig. 5. DSC curves of SP film (A) and NSP film (B).

cross-linking points and restricted the movement of molecular chains. Hence, this resulted in an improved melting temperature of the NSP films.

3.5. SEM analysis

As shown in Fig. 6, the NSP films were smooth and compact, while the SP films had several unequalized holes, suggesting that the miscibility and compatibility in each component in NSP films were increased. Because the surface of the nano-SiO_2 had plenty of unsaturated residual bonds and different hydroxyl group bonding states, it was easy to form a strong hydrogen bond with starch and PVA. The strong chemical bond C–O–Si was also formed in nano-SiO_2/starch/PVA hybrid materials, such that the strong interfacial binding force took place in nano-SiO_2 and starch/PVA, and the film's surface showed a compact and smooth ultrastructure.

3.6. Physical properties

From Table 3, the tensile strength and breaking elongation of the NSP films increased by 79.4% and 18%, respectively, the water absorption decreased by 70%, and the transmittance increased by 15%. The results demonstrated that the miscibility and compatibility between starch and PVA increased with the addition of nano-SiO_2, the secondary crystallization of starch molecules decreased, and then the transmittance, tensile strength, and breaking elongation of the film increased. The network structure formed by combining nano-SiO_2 with starch/PVA, which prevented the water molecules from dissolving, improved the water resistance of the film.

3.7. Biodegradability

The biodegradation rates of NSP films and SP films are shown in Fig. 7. From this figure, it can be seen that the biodegradation rates of NSP films were slightly lower than those of SP films in 100 days, and that the biodegradation rates of the two films were in good coherence after 100 days. That would be because nano-SiO_2 made the miscibility and compatibility increase and form a dense structure between the ST and PVA, which in turn reduced the infiltration velocity of microorganisms. With the increase of degradable time, the compactness of NSP films was destroyed.

Table 3
Effect of nano-SiO_2 on the physical properties of the film

Items	Samples		Change values	Change rates (%)
	SP	NSP		
Tensile strength (MP_a)	10.2	18.3	+8.1	+79.4
Breaking elongation (MP_a)	13.60	16.05	+2.45	+18
Water absorption (%)	48.3	14.5	−33.8	−70
Transmittance (%)	79	91	+12	+15

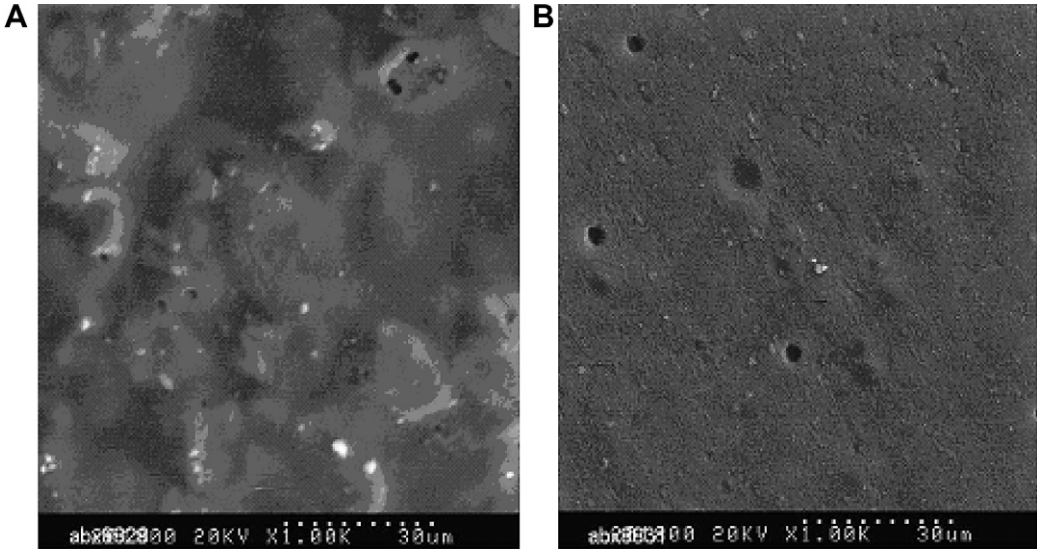

Fig. 6. SEM photographs of SP film (A) and NSP film (B).

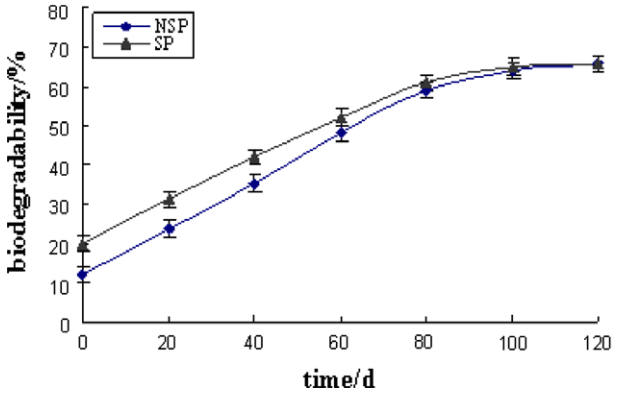

Fig. 7. Biodegradability of SP film and NSP film.

Therefore, the two films exhibited the same degradation rate at a later stage. It was thus indicated that nano-SiO_2 had no influence on the biodegradation rate of the films.

4. Conclusions

The mechanical properties, transmittance, and water resistance of a starch-based full-biodegradable film were all improved significantly with the addition of nano-SiO_2. The film's tensile strength, breaking elongation, and transmittance increased by 79.4%, 18%, and 15%, respectively, and the water absorption decreased by 70%. The biodegradability achieved the requirements of ISO14855:1999.

The permeation took place for the small-size effect and quantum tunneling effect of nano-SiO_2. It was easy to insert in polymer chains and destroy the ordered structure. The intermolecular hydrogen bond was formed in nano-SiO_2 and starch/PVA, and the strong chemical bond C–O–Si was also formed in nano-SiO_2/starch/PVA hybrid materials. Therefore, the miscibility and compatibility were increased and an interpenetrating network structure was formed to prevent the water molecules from dissolving, which greatly increased the water resistance and mechanical properties of the film.

References

Bangyekan, C., Aht-Ong, D., & Srikulkit, K. (2006). Preparation and properties evaluation of chitosan-coated cassava starch films. *Carbohydrate Polymers, 63*, 61–71.

Bikiaris, D., Prinos, J., Koutsopoulos, K., Vouroutzis, N., Pavlidou, E., Frangis, N., et al. (1998). LDPE/plasticized starch blends containing PE-g-MA copolymer as compatibilizer. *Polymer Degradation and Stability, 59*, 287–291.

Chaichana, E., Jongsomjit, B., & Praserthdam, P. (2007). Effect of nano-SiO_2 particle size on the formation of LLDPE/SiO_2 nanocomposite synthesized via the in situ polymerization with metallocene catalyst. *Chemical Engineering Science, 62*, 899–905.

Follain, N., Joly, C., Dole, P., & Bliard, C. (2005). Properties of starch based blends. Part 2. Influence of polyvinyl alcohol addition and photocrosslinking on starch based materials mechanical properties. *Carbohydrate Polymers, 60*, 185–192.

Funke, U., Bergthaller, W., & Lindhauer, M. G. (1998). Processing and characterization of biodegradable products based on starch. *Polymer Degradation and Stability, 59*, 293–296.

Hulleman, Stephan H. D., Janssen, Frank H. P., & Feil, H. (1998). The role of water during plasticization of native starches. *Polymer, 39*, 2043–2048.

Jayasekara, R., Harding, I., Bowater, I., Christie, G. B. Y., & Lonergan, G. T. (2004). Preparation, surface modification and characterisation of solution cast starch PVA blended films. *Polymer Testing, 23*, 17–27.

Lu, Y. S., Tighzerta, L., Dole, P., & Erre, D. (2005). Preparation and properties of starch thermoplastics modified with waterborne polyurethane from renewable resources. *Polymer, 46*, 9863–9870.

Ma, X. F., & Yu, J. G. (2004). The plasticizers containing amide groups for thermoplastic starch. *Carbohydrate Polymers, 57*, 197–203.

Nakamura, E. M., Cordi, L., Almeida, G. S. G., Duran, N., & Mei, L. H. I. (2005). Study and development of LDPE/starch partially biodegradable compounds. *Journal of Materials Processing Technology, 162–163*, 236–241.

Sun, S. S., Li, C. Z., Zhang, L., Du, H. L., & Burnell-Gray, J. S. (2006). Effects of surface modification of fumed silica on interfacial structures and mechanical properties of poly(vinyl chloride) composites. *European Polymer Journal, 42*, 1643–1652.

Xiao, C. M., & Yang, M. L. (2006). Controlled preparation of physical cross-linked starch-g-PVA hydrogel. *Carbohydrate Polymers, 64*, 37–40.

Yang, H., Zhang, Q., Guo, M., Wang, C., Du, R. N., & Fu, Q. (2006). Study on the phase structures and toughening mechanism in PP/EPDM/SiO_2 ternary composites. *Polymer, 47*, 2106–2115.

Yu, L., Dean, K., & Li, L. (2006). Polymer blends and composites from renewable resources. *Progress in Polymer Science, 31*, 576–602.

Zhai, M. L., Yoshii, F., Kume, T., & Hashim, K. (2002). Syntheses of PVA/starch grafted hydrogels by irradiation. *Carbohydrate Polymers, 50*, 295–303.

Zhai, M. L., Yoshii, F., & Kume, T. (2003). Radiation modification of starch-based plastic sheets. *Carbohydrate Polymers, 52*, 311–317.

Zou, W. J., Peng, J., Yang, Y., Zhang, L. Q., Liao, B., & Xiao, F. R. (2007). Effect of nano-SiO_2 on the performance of poly(MMA/BA/MAA)/EP. *Materials Letters, 61*, 725–729.